

Reduced Order Model for enhanced EVAR Planning and navigation guidance

Monica Emendi^{1,3*}, [Eirini Kardampiki](#)^{1,2*}, Karen H. Støverud², Pierluigi di Giovanni³, Sigrid K. Dahl², Aline Bel-Brunon⁴, Victorien Prot⁵, Marco E. Biancolini¹

¹ Department of Industrial Engineering, University of Rome Tor Vergata, Italy

² Department of Health Research, SINTEF Digital, Norway

³ HSL S.r.l, Trento, Italy

⁴ LaMCoS CNRS UMR5259, INSA-Lyon, Villeurbanne F-69621, France

⁵ Department of Structural Engineering, Faculty of Engineering, NTNU, Norway

*These authors equally contributed to the work

1 Introduction

Endovascular aneurysm repair (EVAR) is a minimally invasive procedure for the treatment of abdominal aortic aneurysms that consists in stent graft deployment through the iliac arteries [1]. During this procedure, a stiff guidewire is introduced from the femoral artery towards the aorta to support the proper deployment of the stent graft. The insertion of the stiff wire triggers a straightening effect on the iliac arteries, smoothing out their natural tortuosity [2]. This morphological alteration is hard to be measured intraoperatively or be forecasted preoperatively [3]. The main bottleneck is that the preoperative Computed Tomography (CT) does not get updated during the operation. Consequently, clinicians perform their maneuvers according to the initial aortic configuration and inject contrast in the vessel to visualize their configuration when it is needed. This practice could possibly lead to sub-optimal stent graft sizing, choice of the stent's landing zone and to an increase in radiation exposure and contrast doses, especially in complex cases.

Hence, a real-time prediction of the guidewire path and aortic deformations could be helpful to ease device navigation and reduce post-operative complications. Taking this idea into consideration, this study proposes the generation of a parametric reduced order model for the prediction of aortic deformation in a fast, interactive and user-friendly environment. To this end, morphological, clinical and mechanical features are introduced as input parameters.

To the best of our awareness, this is the first study that combines morphing tools, reduced order models and finite element methods, i.e. LS-DYNA, for this type of clinical application [4].

2 Methodology

The workflow followed in this work is herein presented, starting from the high-fidelity analysis, through its parametrization, to the set-up of the reduced order model. The details of the present work can be found in Emendi, Kardampiki et al. [5].

2.1 High-fidelity parametric analysis

The considered tridimensional model was segmented from CT angiographies of a patient with an abdominal aortic aneurysm by means of an ad-hoc Python script, based on thresholding and morphological algorithms. The obtained mesh was cut, smoothed, and cleaned using Meshmixer (Autodesk, USA), then imported into LS-PrePost processor and re-meshed.

The explicit finite element analysis was set up in LS Pre-Post processor.

The guidewire was discretized with beam elements of size 4 mm. The aortic wall was discretized with triangular shell elements with an average length of 1.4 mm, chosen upon a mesh sensitivity analysis. Linear elastic models for the guidewire and aortic materials were considered for this preliminary study. To simulate the guidewire insertion during EVAR, a velocity curve was imposed on the lowest node of the guidewire. An introducer was considered to avoid the oscillations of the beam outside the aorta. A frictionless contact algorithm (CONTACT_AUTOMATIC_BEAMS_TO_SURFACE), based on soft constraint penalty formulation, was considered in the interaction between the aorta and the guidewire. Further details of the FEM set-up can be found in Emendi et al [6].

The high-fidelity model was automatically parametrized via ad-hoc Python scripts. The following parameters and ranges were considered:

- E_{aorta} , stiffness of the aortic wall, [0.8 – 3] MPa. The range was chosen following (Vallabhaneni et al. 2004) [7]

- E_{wire} , stiffness of the guidewire, [60 – 200] GPa. The minimum value corresponds to the softest guidewire available on the market, Amplatz Super Stiff (Boston Scientific). The maximum value refers to the stiffest commercial guidewire (Cook Medical)
 - ϕ , insertion angle in the sagittal plane, [-25 – 0] °,
 - θ , insertion angle in the frontal plane, [0 – 20] °,
 - α , supra-renal neck angle, [30 – 55] °,
 - β , infra-renal neck angle, [25 – 60] °,
 - τ , tortuosity of left iliac, [0.09 – 0.15], calculated as shown in Fig. 1.
- The last five above-mentioned parameters are illustrated in Fig. 1

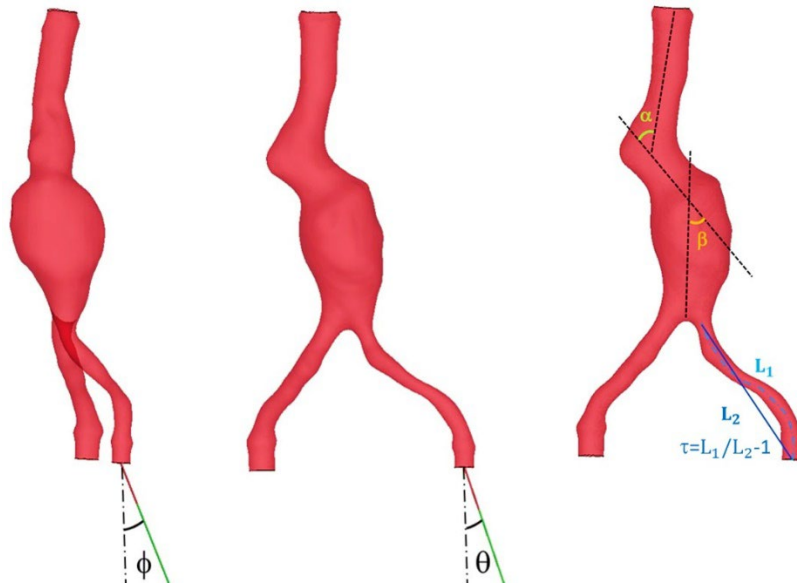


Fig. 1: Illustration of geometrical and morphing parameters: insertion angles in the sagittal and frontal planes ϕ and θ , respectively. Morphing parameters: supra-renal neck angle α , infra-renal neck angle, β and iliac tortuosity, τ .

2.2 Mesh morphing

To vary the parameters α , β and τ , a morphing algorithm based on radial basis functions was applied to the nodes of the aortic mesh. In detail, the Python version of the software RBF Morph (<https://www.rbf-morph.com>) was employed to achieve the desired morphological changes of the model in a fast and automated way. The employed procedure is briefly presented below.

Three sets of source points, \mathbf{x}_n , \mathbf{x}_a and \mathbf{x}_i (located respectively in the neck, aneurysmatic and iliac regions), were selected and a desired displacement was applied to them. These points were used to drive the morphing procedure. Three domains, D_n , D_a and D_i were defined: for each node \mathbf{x} inside these domains the imposed displacement $s(\mathbf{x})$ was calculated as the result of the following interpolating equation:

$$s(\mathbf{x}) = \sum_{i=1}^N \gamma_i \phi(\|\mathbf{x} - \mathbf{x}_{ki}\|) + h(\mathbf{x})$$

Where ϕ are the radial basis functions, γ_i are the weights of the radial basis functions, N is the number of source points, \mathbf{x}_{ki} are the source points and \mathbf{x} the target points, while $h(\mathbf{x})$ is a polynomial whose degree depends on the type of radial basis functions. Further details about the theory of radial basis functions can be found in [8]. The effect of the morphing actions is limited inside the domains.

2.3 Reduced order modeling

The developed ROM was trained with high-fidelity finite element simulation data (i.e. data-driven). The Design of Experiment (DOE) was generated using a Latin Hypercube Sampling algorithm, available on ANSYS DesignXplorer. 300 scenarios were generated varying the above-described parameters and run in batch mode, using 240 cores in parallel (Intel Xeon Gold 6152 CPU @2.10 GHz). The computational time was about 2 hours. The main work that had to be performed was bridging the gap between

LS-DYNA and ANSYS Twin Builder (ANSYS®Electronics Desktop™- Release 22R2) through ad-hoc Python scripts.

The resulting outputs of interest, i.e., the nodal displacement of the aortic wall, were extracted from the simulation results and consequently were converted into binary files, i.e., snapshots, which were then imported in Ansys Twin Builder. The snapshots were divided into training (200 scenarios) and validation sets (100 scenarios), based on the optimal distribution algorithm of Twin Builder. With Singular Value decomposition (SVD), the available data were approximated by a linear combination of 38 snapshots, called modes. Then, a Generic Aggregation Response Surface technique was employed to calculate the value of each mode coefficient in space.

$$\mathbf{d}(\mathbf{x}) = \sum_{i=1}^{38} GARS_i(\mathbf{x}) * mode_i(\mathbf{x})$$

According to this equation, the deformation of a selected point \mathbf{x} in space R^3 is the accumulation of the product of the response surface coefficient and the mode data. Therefore, each ROM prediction contains two errors: deriving from the SVD and the GARS. In this study, we focused on the sum of these two errors, i.e. the final ROM error.

$$e_{ROM} = e_{SVD} + e_{GARS}$$

3 ROM accuracy and deployment

The relative ROM error is below 4.0% for the considered validation scenarios. The absolute ROM error calculated on the magnitude of the nodal displacements is illustrated in Fig. 2. According to statistical analysis, the average final ROM error is estimated equal to 0.3 ± 0.12 mm. The greatest errors, i.e. discrepancies larger than 0.5mm, are detected in 9 scenarios and they occur only in a few nodes. The precision of the current intraoperative imaging modality, i.e. digital subtraction angiography (DSA), is about 0.5 mm. Taking this into consideration, we can conclude that the accuracy of the developed ROM could be sufficient for supporting EVAR planning and navigation.

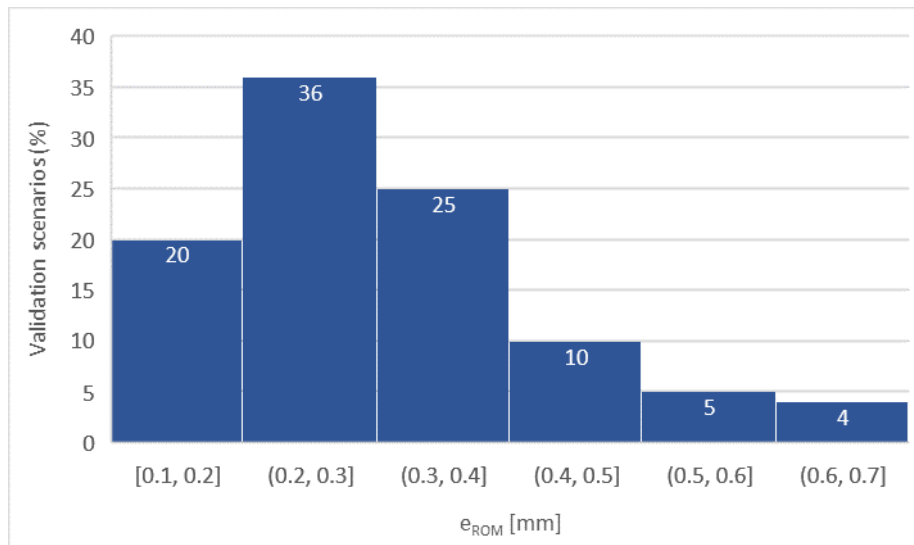


Fig.2: Histogram of the maximum ROM error (mm) detected on the 100 validation scenarios.

As soon as the ROM is built, the results can be obtained almost in real-time. In Fig. 3, the ANSYS ROM interactive Graphical User Interface (GUI) environment is shown. The user can tune the aforementioned parameters on the input parameters' panel. Then within some seconds, the ROM result is presented on the main panel of the screen. For each ROM prediction, an estimation of the ROM error is calculated according to the interpolation of the learning data error.

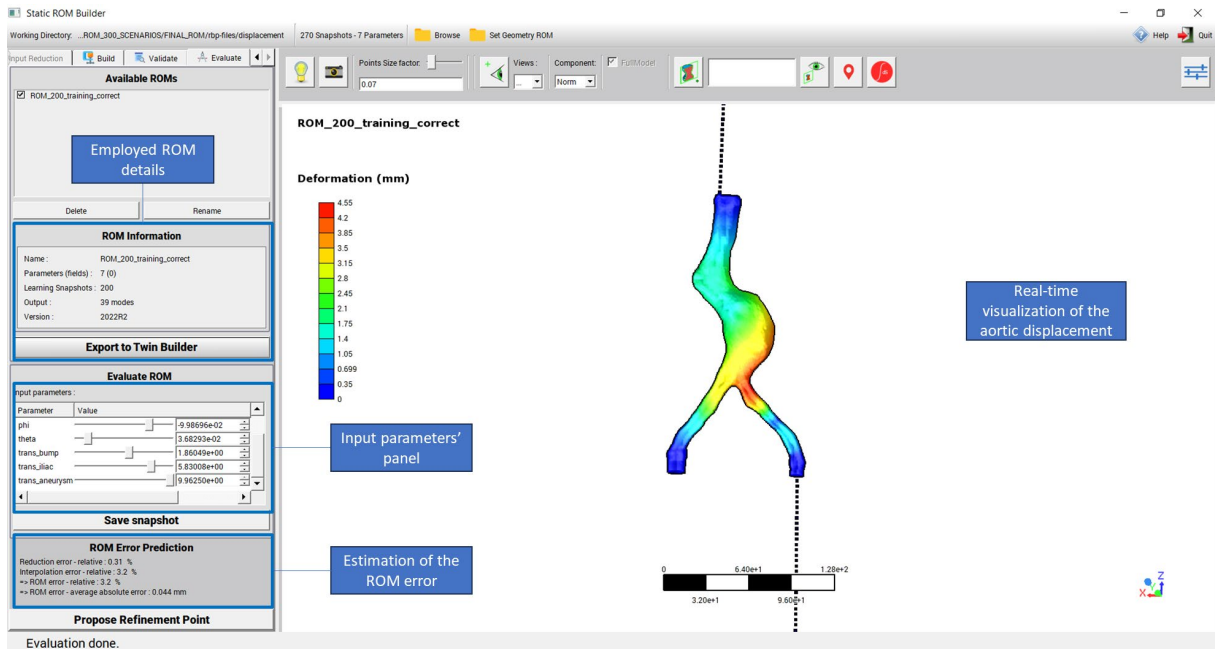


Fig.3: ANSYS Twin Builder interactive Graphical User Interface environment which contains the input parameters' panel, the estimation of ROM error panel and the main screen showing in real-time the aortic displacement.

In order to appreciate the value of the developed pipeline, below we compare the timeframe of calculating the aortic deformation with Finite Element Software, i.e. LS-DYNA and the ROM trained on Finite Element data. The proposed workflow speeds up the displacement calculation by two means. According to Fig. 4, acquiring a patient-specific geometrical model requires 45 minutes whereas morphing a baseline geometry to a patient-specific one takes 6 seconds, provided that the RBF modifiers are tuned. The time needed for the set-up of the RBF modifiers depends from the user's skills and familiarity with the software but the whole process is simple. The second advantage of the proposed approach is that the computational cost of building up a ROM, i.e. 165 minutes, has to be paid once and then every ROM prediction is offered almost in real-time. On the other hand, the FEM solution demands 25 minutes and every change in the input parameters results in a new FEM calculation. Hence, the developed ROM can be perceived as an efficient and systematic way of learning from FEM data.

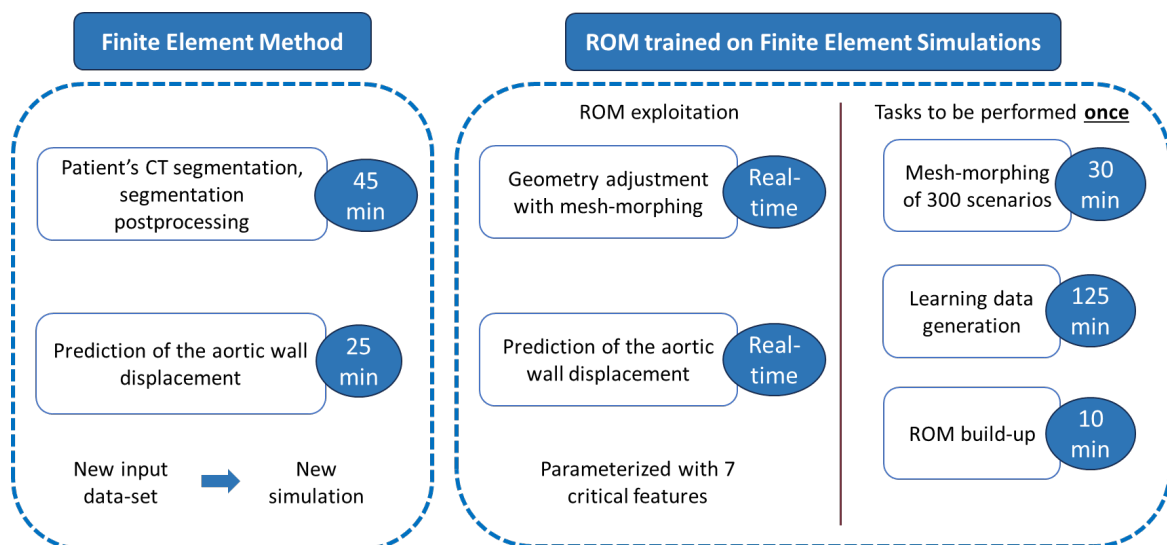


Fig.4: Comparison of the timeframes that characterize the pipelines of high-fidelity analysis and reduced order modeling.

4 Summary

EVAR pre-operative planning and navigation guidance is currently challenged by the abdominal aortic deformation which is triggered by the insertion of stiff guidewire. Nowadays, clinicians operate with the support of imaging fusion techniques, DSA and fluoroscopy but still there is a mismatch between the pre-operative CT and the intra-operative aortic configuration. High-fidelity Finite Element simulations can predict the aortic wall deformations, but they are time-demanding, thus not compliant with the clinical timeframe. Towards overcoming this obstacle, we developed a parametric Reduced Order Model which predicts the aortic motion as a function of seven critical parameters. The accuracy of the proposed ROM was found to be sufficient with respect to the resolution of the currently used imaging technologies. The ROM response was provided within some second, showing potential of being employed pre- and intra-operatively. Additional research on further reducing the ROM error seems a captivating upcoming challenge, as well as applying the proposed workflow to a more complex vascular geometry.

5 Acknowledgements

The research has received funding from the European Union's Horizon 2020 research and innovation programme under the Marie Skłodowska-Curie grant agreement No 859836, MeDiTATe: "The Medical Digital Twin for Aneurysm Prevention and Treatment".

6 Literature

- [1] G. S. Oderich, Ed., *Endovascular Aortic Repair*. Cham: Springer International Publishing, 2017. doi: 10.1007/978-3-319-15192-2.
- [2] H. O. Kim, N. Y. Yim, J. K. Kim, Y. J. Kang, and B. C. Lee, 'Endovascular Aneurysm Repair for Abdominal Aortic Aneurysm: A Comprehensive Review', *Korean J. Radiol.*, vol. 20, no. 8, p. 1247, 2019, doi: 10.3348/kjr.2018.0927.
- [3] A. Kaladji *et al.*, 'Prediction of deformations during endovascular aortic aneurysm repair using finite element simulation', *Comput. Med. Imaging Graph.*, vol. 37, no. 2, pp. 142–149, Mar. 2013, doi: 10.1016/j.compmedimag.2013.03.002.
- [4] J. Gindre *et al.*, 'Finite element simulation of the insertion of guidewires during an EVAR procedure: example of a complex patient case, a first step toward patient-specific parameterized models: FE Simulation of the Insertion of Endovascular Guidewires', *Int. J. Numer. Methods Biomed. Eng.*, vol. 31, no. 7, p. e02716, Jul. 2015, doi: 10.1002/cnm.2716.
- [5] M. Emendi, E. Kardampiki *et al.*, 'Towards a reduced order model for EVAR Planning and intra-operative navigation. Manuscript submitted for publication.
- [6] M. Emendi *et al.*, 'Prediction of guidewire-induced aortic deformations during EVAR: a finite element and in vitro study', *Front. Physiol.*, vol. 14, p. 1098867, Jul. 2023, doi: 10.3389/fphys.2023.1098867.
- [7] S. R. Vallabhaneni, G. L. Gilling-Smith, T. V. How, S. D. Carter, J. A. Brennan, and P. L. Harris, 'Heterogeneity of Tensile Strength and Matrix Metalloproteinase Activity in the Wall of Abdominal Aortic Aneurysms', *J. Endovasc. Ther.*, vol. 11, no. 4, pp. 494–502, Aug. 2004, doi: 10.1583/04-1239.1.
- [8] M. E. Biancolini, *Fast radial basis functions for engineering applications*. Springer, 2017.